In vivo analysis of undocked connexin43 gap junction hemichannels in ovarian granulosa cells

Dan Tong[1,2,3,4], Tony Y. Li[1,2,3,4], Kathryn E. Naus[1,2,3,4], Donglin Bai[1] and Gerald M. Kidder[1,2,3,4,*]

Departments of [1]Physiology and Pharmacology, [2]Obstetrics and Gynecology and [3]Paediatrics, Schulich School of Medicine and Dentistry, The University of Western Ontario, London, ON N6A 5C1, Canada
[4]Children's Health Research Institute, 800 Commissioners Road East, London, ON, Canada
*Author for correspondence (e-mail: gerald.kidder@schulich.uwo.ca)

Accepted 3 September 2007
Journal of Cell Science 120, 4016-4024 Published by The Company of Biologists 2007
doi:10.1242/jcs.011775

Summary

Connexin43 (Cx43, encoded by *Gja1*) is required for ovarian follicle development in the mouse. It is strongly expressed in granulosa cells, in which it forms intercellular gap junction channels that couple the cells metabolically. However, recent evidence indicates that undocked gap junction hemichannels can also have physiological roles such as mediating the release of small messenger molecules, including ATP. In this study, the presence of undocked Cx43 hemichannels in granulosa cells was revealed by dye uptake induced either by mechanical stimulation or by the reduction of extracellular divalent cations, both of which are known triggers for hemichannel opening. ATP release was also detected, and could be abolished by connexin-channel blockers. None of these putative hemichannel-mediated activities were detected in Cx43-deficient granulosa cells. Therefore, we hypothesized that hemichannels account for the essential role of Cx43 in folliculogenesis. To test this, a Cx43 mutant lacking the conserved cysteines on the extracellular loops (cys-less Cx43), reported to form hemichannels but not intercellular channels, was retrovirally expressed in Cx43-deficient granulosa cells. The infected cells were then combined with wild-type oocytes to make reaggregated ovaries, which were grafted into host kidneys. Although re-introduction of wild-type Cx43 rescued folliculogenesis, introduction of cys-less Cx43 did not. Therefore, although Cx43 gap junction hemichannels might play a role in ovarian folliculogenesis, their contribution does not supplant the need for intercellular gap junction channels.

Key words: Oogenesis, Folliculogenesis, Undocked connexons

Introduction

Gap junctions are specialized cell-to-cell channels that enable neighboring cells to exchange small signaling molecules (less than ~1 kDa), and to synchronize metabolic and electrical activities. Each gap junction channel is composed of two hemichannels or connexons that reside in the plasma membrane of two closely apposed cells and dock with each other via their extracellular domains. Hemichannels are hexamers of protein subunits, members of a family of homologous proteins called connexins. To date, 20 and 21 connexin genes have been found in the mouse and human genomes, respectively (reviewed by Söhl and Willecke, 2004).

Although once considered to represent nothing more than an intermediate step in gap junction assembly (Li et al., 1996), undocked hemichannels are now understood to play a variety of physiological and pathological roles. Recent studies have documented that undocked hemichannels can open on the non-junctional cell surface in response to membrane depolarization, mechanical stimulation, metabolic stress, reduction in extracellular calcium and an increase of cytoplasmic calcium (reviewed by Bennett et al., 2003; Goodenough and Paul, 2003; De Vuyst et al., 2006). Hemichannels are involved in a number of cellular processes, including: the release of ATP, NAD^+, prostaglandin and glutamate (Stout et al., 2002; Ye et al., 2003; Bruzzone et al., 2001; Cherian et al., 2005; Zhao et al., 2005); intercellular calcium wave propagation (Stout et al., 2002); cell-volume regulation (Quist et al., 2000); and transduction of survival signals (Plotkin et al., 2002). However, because all these studies were performed in vitro, it is not clear whether gap junction hemichannels play physiological roles in vivo.

Ovarian follicles have provided fertile ground for exploring the physiological roles of gap junctional communication (reviewed by Kidder, 2005). Connexin43 (Cx43, encoded by *Gja1*) is highly expressed in developing follicles, in which it forms the gap junctions coupling granulosa cells (Gittens et al., 2003; Tong et al., 2006). The indispensable role of this connexin during ovarian folliculogenesis has been clearly demonstrated using knockout mice. In C57BL/6-strain *Gja1*-knockout mice ($Gja1^{-/-}$), folliculogenesis is arrested in the primary stage and the oocytes are developmentally incompetent (Ackert et al., 2001). This impairment is related to the fact that granulosa cells lacking Cx43 display a lower proliferation rate and a reduced response to an oocyte-derived mitogen, indicating an impaired granulosa cell function and not an oocyte defect as the primary cause (Gittens et al., 2005; Gittens and Kidder, 2005).

None of the studies published to date on Cx43 in granulosa cells have ruled out the possibility that gap junction hemichannels and not intercellular gap junction channels account for its indispensable role in folliculogenesis. Indeed, there is information in the literature suggesting a possible role for undocked hemichannels in folliculogenesis. Studies have shown, for example, that extracellular ATP can act through P2 purinergic receptors to induce Ca^{2+} oscillation within granulosa cells (Tai et al., 2000), thus potentially regulating their activities, such as secretion, differentiation, proliferation

and apoptosis (Lara et al., 2001; Flores et al., 1998; Kamada et al., 1995; Park et al., 2003). Furthermore, ATP-induced Ca^{2+} release in granulosa cells can lead to an increase in Ca^{2+} level in the oocyte, suggesting a possible role for this nucleotide as an important messenger within the developing follicle (Webb et al., 2002). Because undocked Cx43 hemichannels have been demonstrated to mediate the release of ATP in many other cell types, these findings suggest that they might function similarly in ovarian granulosa cells and could be required for follicular development.

The experiments carried out in the present study were designed to test the hypothesis that undocked gap junction hemichannels composed of Cx43 exist in mouse granulosa cells and are involved in folliculogenesis. The presence of undocked Cx43 hemichannels was explored by comparing the hemichannel properties of wild-type and Cx43-deficient granulosa cells. The essential involvement of undocked Cx43 hemichannels in folliculogenesis was tested in vivo by retroviral delivery of a hemichannel-only Cx43 construct [Cx43 lacking the conserved cysteines of the extracellular loops (Bao, X. et al., 2004)] into Cx43-deficient granulosa cells, which were then combined with oocytes to construct reaggregated ovaries. Our results demonstrate that, although undocked Cx43 hemichannels are present in ovarian granulosa cells, they alone cannot support follicular development.

Results

Dye uptake and ATP release by granulosa cells

To look for the presence of undocked hemichannels in the plasma membranes of mouse granulosa cells, we performed dye-uptake assays on primary cultures of cell monolayers using the low-molecular-weight fluorescent dyes Lucifer yellow (LY, 457 Da) and propidium iodide (PI, 668 Da), which are not membrane permeable but can pass through gap junction hemichannels (Gomes et al., 2005; Lai et al., 2006). In regular extracellular solution, both wild-type (3.4±0.4%, n=4 with a total of 178 cells being counted) and Cx43-deficient (2.6±0.3%, n=4, total of 180 cells) cells showed minimal dye uptake (Fig. 1A,D). After removing extracellular Ca^{2+} and Mg^{2+}, wild-type granulosa cells showed significant uptake of LY (72.0±9.2%, n=6, total of 278 cells) (Fig. 1B,D); a similar result was obtained when calcium alone was removed from the medium (data not shown). By contrast, very few Cx43-deficient granulosa cells were loaded with dye under the Ca^{2+}- and Mg^{2+}-free condition (4.5±3.7%, n=5, total of 194 cells) (Fig. 1D). This difference between wild-type and Cx43-deficient granulosa cells was not an artifact due to gap junctional sharing of dye between the wild-type cells, because the same result was obtained when very-low-density cultures were used (data not shown). Dye uptake by wild-type granulosa cells was significantly blocked by previously reported hemichannel blockers: carbenoxolone (CBX, 200 μM; Fig. 1C), flufenamic acid (FFA, 100 μM) and mefloquine (MFQ, 50 μM) (P<0.001 for each compared to the blocker-free condition; Fig. 1D), indicating that undocked Cx43 connexons mediated the dye uptake under the extracellular divalent-cation-free (DCF) condition. For carbenoxolone, a concentration-inhibition experiment revealed that a concentration of at least 100 μM was required to significantly inhibit LY uptake (data not shown). These results are consistent with previous studies showing that removal of extracellular divalent cations can open gap junction hemichannels (Stout et al., 2002; Zhao et al., 2005; Lai et al., 2006; De Vuyst et al., 2007). To exclude the possible involvement of the large pore-forming channel P2X7 receptor (also known as P2RX7) (Suadicani et al., 2006), the

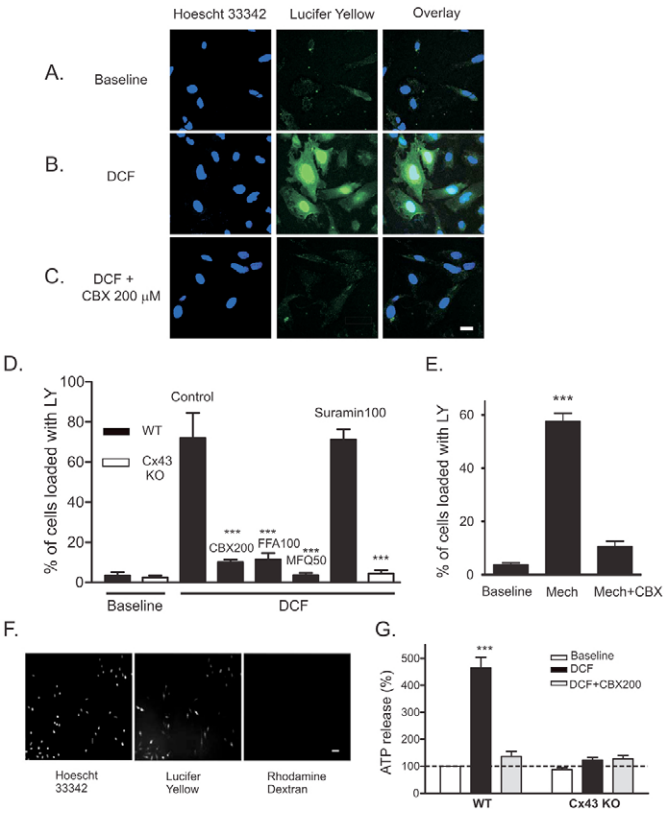

Fig. 1. The presence of undocked Cx43 hemichannels in mouse granulosa cells demonstrated by Lucifer yellow (LY) dye uptake or ATP release triggered by divalent-cation-free (DCF) solution or mechanical stimulation. (A-C) Representative experiments show LY uptake by wild-type granulosa cells in regular extracellular solution (A), DCF solution (B) or DCF solution with 200 μM carbenoxolone (CBX; C). The left column shows blue nuclear staining with Hoechst 33342, the middle column shows intracellular green fluorescence resulting from the uptake of LY and the right column shows the overlay. Scale bar, 10 μm. (D) Quantitative data, expressed as the percentage of cells loaded with LY relative to the total number of cells in a field of view, counted after Hoechst staining (mean ± s.e.m. of four to six different coverslips under each condition) of wild-type (WT) or Cx43-deficient (Cx43-KO) cells. (E) The data are plotted as the percentage of cells loaded with LY relative to the total number of cells in the field of view (mean ± s.e.m. of three to four different coverslips under each condition) after mechanical stimulation (mech). See Results for the blockers used. (D,E) ***P<0.001 versus baseline (one-way ANOVA and Tukey's post-hoc test).
(F) Representative experiments show LY (middle) and rhodamine dextran (bottom) uptake by wild-type granulosa cells after mechanical stimulation. Cell numbers were counted by nuclear staining with Hoechst 33342 (top). Scale bar, 50 μm. (G) Data represent ATP release by wild-type and Cx43-deficient (Cx43-KO) granulosa cells triggered by DCF solution with or without 200 μM CBX. The data were normalized to baseline value (wild-type cells in regular ECS, broken line). ***P<0.001 versus baseline (two-way ANOVA and Bonferroni post-hoc test).

nonselective purinergic-receptor blocker suramin (IC_{50}=5 μM for blocking pore formation of the rat P2X7 receptor) (Hibell et al., 2001) was used. Suramin (100 μM) failed to block the dye loading of wild-type granulosa cells (71.2±6.8%, *n*=5, total of 221 cells; *P*>0.05 compared to the blocker-free condition) (Fig. 1D). Furthermore, mechanical stimulation, another widely used condition to induce opening of hemichannels (Zhao et al., 2005; Cherian et al., 2005), also triggered significant (*P*<0.001) dye uptake by wild-type granulosa cells (57.5±0.8%, *n*=4, total of 464 cells) as compared with non-stimulated cells (3.7±0.4%, *n*=3, total of 178 cells). Again, the effect could be blocked by CBX (200 μM) (10.6±0.6%, *n*=3, total of 265 cells; *P*<0.01 versus mechanical stimulation only) (Fig. 1E). Because uptake of rhodamine-labeled dextran, a molecule too large (10 kDa) to pass through gap junction hemichannels, did not occur after mechanical stimulation, the LY uptake was not due to cell membrane damage (Fig. 1F).

Incubation of granulosa cells in DCF solution also triggered a 4.6±0.4-fold increase in ATP release compared with controls; this increase was significantly above the baseline (*P*<0.001) (*n*=17) and was significantly suppressed by CBX (*P*>0.05 compared with baseline) (*n*=16) (Fig. 1G). By contrast, Cx43-deficient granulosa cells did not show a significantly increased ATP release under the DCF condition, and CBX had no obvious effect either (*n*=10 each) (Fig. 1G, *P*>0.05 compared with baseline). Collectively, these results indicate that undocked Cx43 hemichannels on granulosa cells open in response to reduced extracellular divalent cations and release ATP.

Expression of pannexins and P2X7 receptors

It has been reported that activation of pannexin channels provides another pathway for dye uptake and ATP release (Bao, L. et al., 2004; Pelegrin et al., 2006; Suadicani et al., 2006). To exclude the possibility that the difference we observed between wild-type and Cx43-deficient granulosa cells was mediated by these channels, we analyzed the expression of genes encoding pannexins. By reverse transcriptase (RT)-PCR, we detected transcripts encoding all three pannexins in RNA from whole ovary, but only pannexin 1 (*Panx1*) mRNA was detected in granulosa cells (Fig. 2A). Semi-quantitative RT-PCR demonstrated that *Panx1* expression remained constant in the granulosa cells during follicular development from the fetal (gestation day 18.5) to mature (3- to 4-weeks old) stage (*P*>0.05, Fig. 2B). Furthermore, there was no significant difference in *Panx1* expression between wild-type and Cx43-deficient granulosa cells (*P*>0.05, Fig. 2B,C). The same result was obtained when *P2rx7* gene expression was analyzed in the same way. These data, along with the suramin-treatment result described above and the relative insensitivity of hemichannel opening to carbenoxolone as compared with that of pannexin channels (5 μM) (Huang et al., 2007), indicate that neither P2X7 receptors nor pannexin channels are likely candidates to mediate the observed ATP release/dye uptake in granulosa cells.

Characterization of cys-less Cx43 in MDCK cells and granulosa cells

It has been shown that the highly conserved cysteine residues located in the extracellular loops of the connexins are essential

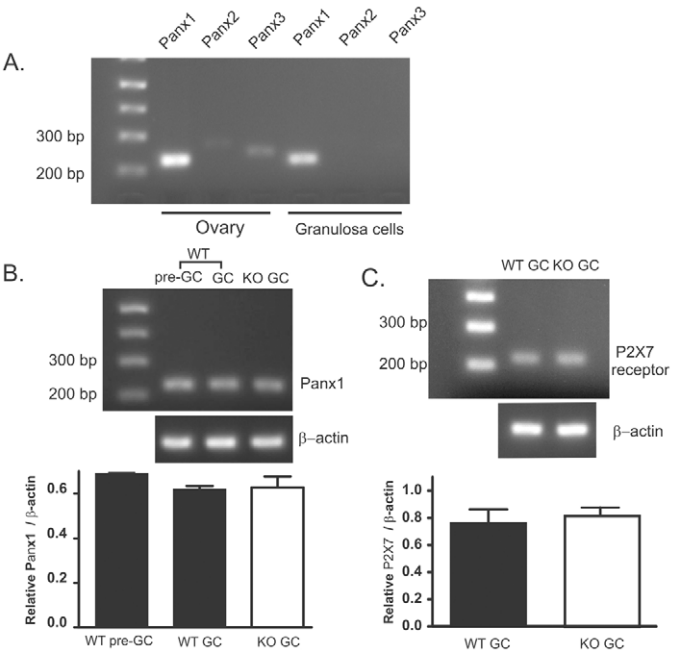

Fig. 2. RT-PCR analysis of the mRNAs encoding pannexins and the P2X7 receptor from whole ovary and granulosa cells. (A) Representative results of the analysis for *Panx1*, *Panx2* and *Panx3* transcripts. (B) Semiquantitative measurement of *Panx1* transcripts in granulosa cells from wild-type (WT) fetuses (E18.5, WT pre-GC), wild-type 3- to 4-week-old mice (WT GC) and Cx43-deficient ovaries 3-4 weeks after grafting into adult kidney capsules (KO GC). The bar graph (bottom) shows the average relative amplicon band intensity (*Panx1*:*Actb* amplicon ratio), which was determined by densitometry (*n*=4; *P*>0.05, one way ANOVA). (C) Similarly, semiquantitative RT-PCR was used to compare *P2rx7* transcript levels in wild-type and Cx43-deficient granulosa cells (*n*=4; *P*>0.05, unpaired *t*-test).

for the docking of hemichannels with each other to form intercellular gap junction channels (Dahl et al., 1991). Cx43 lacking all six cysteines on its extracellular loops is unable to form functional gap junction channels, but still retains hemichannel functions, as determined from experiments with *Xenopus* oocytes (Bao, X. et al., 2004). To further characterize this mutant protein in mammalian cells, we produced the cys-less Cx43 construct by mutating the six cysteines on the extracellular loops to alanines (Fig. 3A,B). The construct also included an enhanced green fluorescent protein (EGFP) cassette as a reporter downstream of an internal ribosomal entry site (IRES). In preliminary experiments, the cys-less Cx43 construct was retrovirally delivered into Madin-Darby canine kidney (MDCK) cells, which retain a minimal level of endogenous intercellular coupling when they are confluent (Cereijido et al., 1984). To confirm that the cys-less Cx43 constructs were integrated into the cell genome, the cells were passaged for 4 weeks after retroviral infection. We found that more than 90% of infected MDCK cells still showed EGFP expression after 4 weeks, indicating that the constructs were stably integrated into the cell genome. Immunostaining showed that the cys-less Cx43 could be detected on the cell membrane, although much of it was intracellular. However, in contrast to the extensive dye transfer between infected cells mediated by

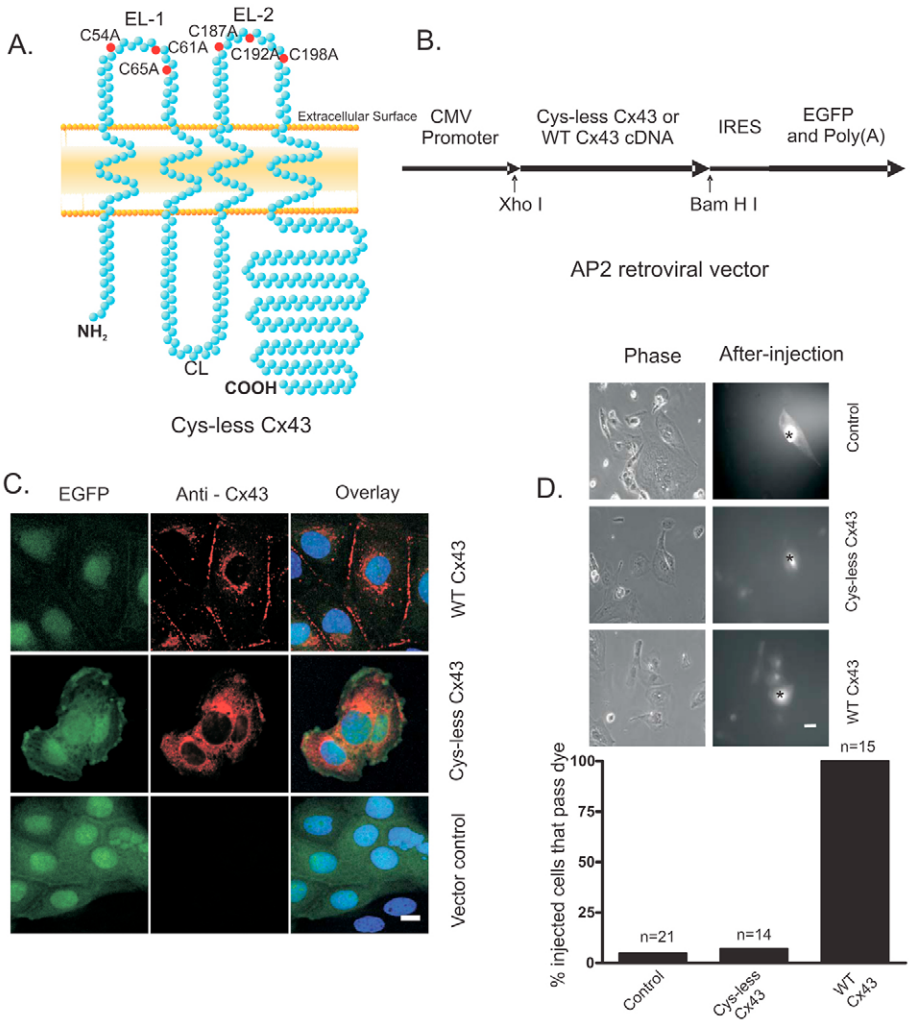

Fig. 3. Cys-less Cx43 structure, expression and function in Cx43-deficient granulosa cells. (A) Cx43 protein structure showing the six cysteine sites (red) on the extracellular loops that were mutated to form cys-less Cx43. (B) Schematic structure of the AP2 retrovector showing the segment encoding either cys-less Cx43 or wild-type Cx43 followed by an IRES-linked sequence encoding EGFP. The vector control contained only the IRES and the EGFP sequence. (C) Expression of wild-type (WT) Cx43 and cys-less Cx43 in Cx43-deficient granulosa cells. Infected cells were identified by EGFP expression (left column). Cx43 immunostaining showed mainly membrane expression of wild-type Cx43 with numerous gap junction-like plaques, and both membrane and cytoplasmic localization of cys-less Cx43. The overlay is shown in the right column. (D) Representative experiments showing the transfer of LY to neighboring cells after microinjection into one cell (asterisk) among the three treatment groups. Quantification of dye transfer (percentage of cells passing injected LY to more than one neighboring cell) is shown in the bar graph. The number of cells injected is shown above each bar. Scale bars, 10 μm.

wild-type Cx43, the cys-less Cx43 bestowed very limited intercellular dye-transfer ability (Table 1), demonstrating that cys-less Cx43 lacks the ability to form functional intercellular gap junction channels.

Having thus confirmed the ability of the cys-less Cx43 construct to be stably expressed, the same construct was introduced into Cx43-deficient fetal pre-granulosa cells by retroviral delivery. By immunostaining, cys-less Cx43 expression was located on the cell plasma membrane as well as in the cytoplasm (Fig. 3C). Similar to what was observed in the MDCK cells, cys-less Cx43 was not able to confer intercellular dye-transfer ability on Cx43-deficient granulosa cells, whereas wild-type Cx43 was (7.1%, n=14 versus 100%, n=15, respectively) (Fig. 3D). To test for gap junction hemichannel function, the infected granulosa cells were exposed to DCF solution and both dye-uptake and ATP-release assays were performed. To better distinguish the test dye from the reporter EGFP, PI was used in the dye-uptake assay instead of LY (Fig. 4A). As plotted in Fig. 4B, granulosa cells expressing cys-less Cx43 showed a significant increase in dye uptake when exposed to DCF solution (84.3±9.1%, n=3, total of 80 cells counted) compared with the same cells in regular solution (3.2±0.6%, n=3, total of 93 cells). Similarly, 82.4±15.1% of cells infected with wild-type Cx43 showed dye uptake in DCF (n=3, total of 78 cells) compared with 2.2±0.3% of cells in regular solution (n=3, total of 81 cells). This dye uptake was blocked by CBX (200 μM, Fig. 4B). Furthermore, granulosa cells infected with either wild-type Cx43 or cys-less Cx43 showed a significant increase in DCF-triggered ATP release (Fig. 4C; fold increase of 6.3±1.2 and 7.0±1.4, respectively; P<0.001 compared with regular extracellular solution), demonstrating that cys-less Cx43 can form functional gap junction hemichannels in granulosa cells despite its inability to form functional intercellular channels. Because

Table 1. Ability of connexin constructs to confer Lucifer yellow dye coupling on infected MDCK cells

Construct	Number of injected cells	Number of cells passing dye	% dye coupled	Extent of dye transfer (number of recipient cells)
Wild-type Cx43	52	43	83	>3
Cys-less Cx43	80	12	15	1
Vector control	50	5	10	1

the levels of both dye uptake and ATP release were similar between cells infected with wild-type or cys-less Cx43, we were confident that the levels of expression of the two connexins were comparable.

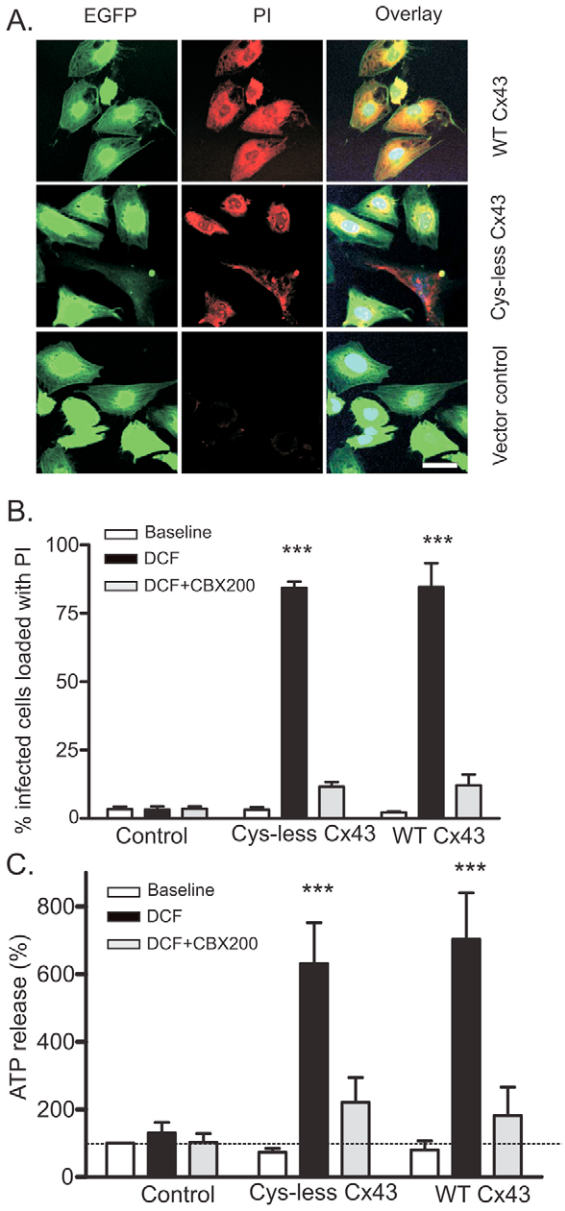

Fig. 4. Comparison of wild-type and cys-less Cx43 hemichannel function in granulosa cells. (A) Propidium iodide (PI) uptake (red, central column) of Cx43-deficient granulosa cells infected with wild-type (WT) Cx43 (top row), cys-less Cx43 (middle row) or control vector (bottom row) under DCF conditions. Scale bar, 20 μm. (B) Quantification of PI uptake (percentage of EGFP-expressing cells loaded with PI) in regular ECS (baseline), in DCF solution or in DCF solution with 200 μM CBX in the three cell types, as shown under each group of bars. Data are expressed as mean ± s.e.m. of three to four different experiments under each condition. (C) Quantification of ATP release by Cx43-deficient granulosa cells infected with wild-type Cx43, cys-less Cx43 or control vector under regular ECS, DCF solution or DCF solution with 200 μM CBX. All data were normalized to baseline value (wild-type cells under regular ECS, broken line). n=4, 4 and 3 for the three cell groups, respectively. (B,C) ***P<0.001 versus control (two-way ANOVA and Bonferroni post-hoc test).

Folliculogenesis in reaggregated ovaries expressing cys-less Cx43

To test the hypothesis that undocked hemichannels, by themselves, can fulfill the essential role of Cx43 in granulosa cells, we constructed ovaries using Cx43-deficient pre-granulosa cells retrovirally infected with different DNA constructs (wild-type Cx43, cys-less Cx43 or empty vector lacking any connexin cDNA). These genetically modified granulosa cells were combined with wild-type oocytes to form cell pellets. The cell pellets were transplanted under the kidney capsules of adult host females, allowing us to observe follicular development in vivo. In reaggregated ovaries made with wild-type oocytes and Cx43-deficient granulosa cells infected with wild-type Cx43, follicles of all developmental stages were observed (Fig. 5A,B), indicating that the virally re-introduced wild-type Cx43 had rescued the impaired folliculogenesis of Cx43-null mutant ovaries. However, ovaries made with Cx43-deficient granulosa cells infected with cys-less Cx43 only contained follicles at early stages (Fig. 5A,B), similar to what was observed in the empty-vector control group and in the grafted Cx43-null mutant ovaries reported previously (Ackert et al., 2001). The follicle distributions were significantly different between ovaries expressing wild-type Cx43 and those expressing cys-less Cx43 (P<0.001, chi-square test) as well as between ovaries expressing wild-type Cx43 and those infected with empty vector (P<0.01, chi-square test). No statistical difference was observed between the distribution in cys-less Cx43-infected ovaries and empty-vector-infected ovaries (P>0.05) (total follicles=72, 33 and 22 from three, four and three reaggregated ovaries expressing wild-type Cx43, cys-less Cx43 or empty vector, respectively). Immunostaining confirmed the expression of the introduced constructs in the reaggregated ovaries (Fig. 5C). Similar to what was observed immediately after infection, cys-less Cx43 in the reaggregated ovaries after 4 weeks showed strong intracellular expression, whereas wild-type Cx43 mainly formed plaque-like structures between granulosa cells. As a negative control, no Cx43 was detected in ovaries infected with empty vector. These results strongly indicate that cys-less Cx43 cannot rescue the folliculogenesis defect caused by the loss of Cx43 from granulosa cells.

Discussion

Numerous studies have indicated that, in addition to forming intercellular gap junction channels, connexons can function as undocked hemichannels and in other ways, involving interactions with other proteins (reviewed by Jiang and Gu, 2005). Undocked hemichannels are involved in the release of important signaling molecules, including ATP, NAD^+, prostaglandin and glutamate (Stout et al., 2002; Ye et al., 2003; Bruzzone et al., 2001; Cherian et al., 2005; Zhao et al., 2005), suggesting possible roles for gap junction hemichannels in paracrine signaling. Previous studies with Cx43-knockout mice demonstrated an essential role for this connexin in ovarian granulosa cells in supporting folliculogenesis and the development of competent oocytes (Ackert et al., 2001; Gittens et al., 2003; Gittens et al., 2005). Although the loss of Cx43 from granulosa cells abolished gap junctional intercellular

communication (Gittens et al., 2003; Tong et al., 2006), no evidence has been presented that it is the loss of intercellular channels and not hemichannels, or both, that accounts for the ovarian defects. Given the presence of various purinergic receptors on granulosa cells (Tai et al., 2000) and the possible role of ATP signaling in regulating the meiotic activity of oocytes (Webb et al., 2002), it was important to investigate the possibility that Cx43 functions only as undocked hemichannels during follicular development.

In the present study, the presence of undocked Cx43 hemichannels in granulosa cell plasma membranes was demonstrated by measuring dye uptake and ATP release triggered by removing extracellular divalent cations or by mechanical stimulation, two common ways to induce the opening of gap junction hemichannels in various cell types (Stout et al., 2002; De Vuyst et al., 2007; Zhao et al., 2005; Cherian et al., 2005). Both dye uptake and ATP release were inhibited by various gap junction hemichannel blockers and were absent in Cx43-deficient granulosa cells, indicating that both phenomena were due to hemichannels composed of Cx43. By contrast, our results indicated that pannexins and P2X7 receptors, both of which have been reported to form pore-like channels in the cell membrane (Bao, L. et al., 2004; Pelegrin et al., 2006; Suadicani et al., 2006), are not involved because there was no change in either *Panx1* or *P2rx7* gene expression with the loss of Cx43, the sensitivity of hemichannel-mediated LY uptake to carbenoxolone was much lower than that of pannexin channels (5 μM) (Huang et al., 2007) and there was no effect of a P2X7-receptor antagonist on dye uptake. Collectively, these results support the conclusion that undocked Cx43 hemichannels are present in granulosa cells and can be induced to open under mechanical stress or a reduced extracellular level of divalent cations to allow ATP release. In rapidly growing follicles, granulosa cells might be subjected to mechanical deformation due to their frequent cell division, growth of the oocyte and/or expansion of the fluid-filled antrum during later stages. Furthermore, the ionic concentration of the antral fluid, to which the granulosa cells are exposed, changes dynamically during follicular development (Nandi et al., 2006), another possible cause of hemichannel opening and ATP release.

To distinguish between the potential roles of Cx43 in forming gap junction channels and hemichannels in granulosa cells, we took advantage of a hemichannel-only Cx43 construct. It has been reported that mutant Cx43 lacking the conserved six cysteines in the extracellular loops cannot form functional gap junction channels, but still maintains hemichannel function, as revealed in *Xenopus* oocytes by the dye-uptake assay (Bao, X. et al., 2004). We confirmed this in mammalian cells by retrovirally delivering the cys-less Cx43 construct into either MDCK cells or into Cx43-deficient fetal granulosa cells, neither of which exhibit gap

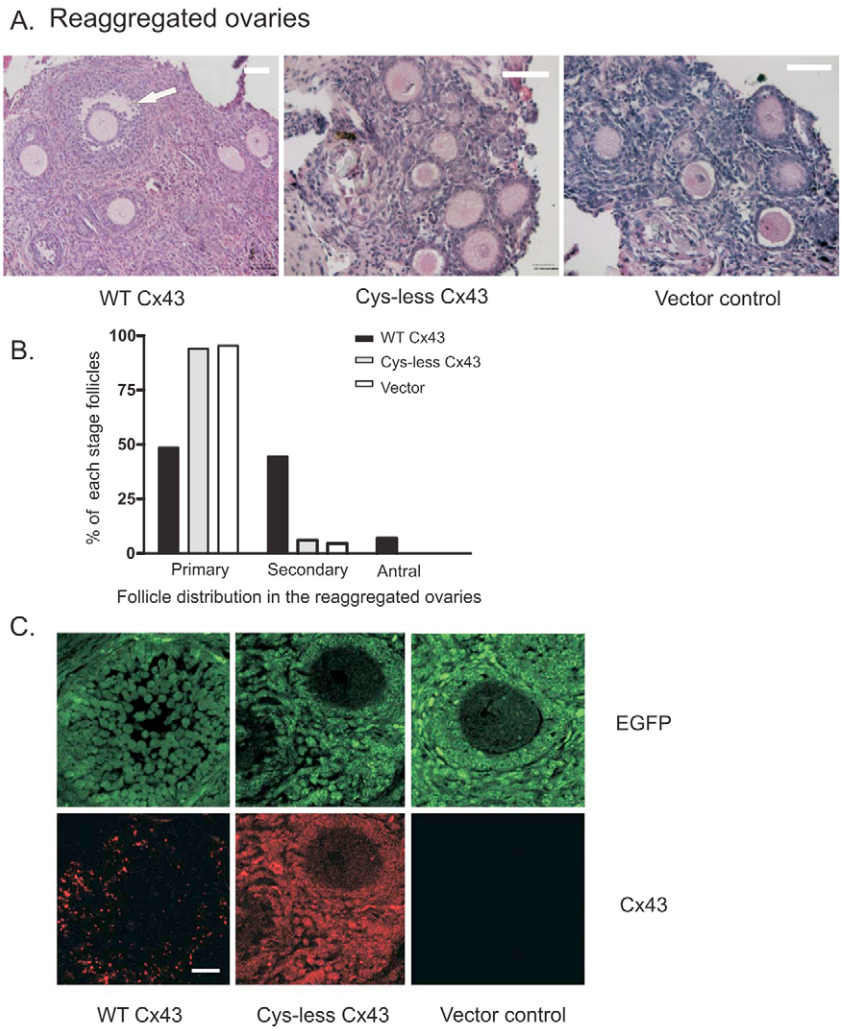

Fig. 5. Folliculogenesis in reaggregated ovaries. (A) In ovaries constructed with Cx43-deficient granulosa cells infected with wild-type (WT) Cx43, follicles of all developmental stages were observed (left; white arrow points to an antral follicle), whereas, in ovaries constructed with Cx43-deficient granulosa cells infected with cys-less Cx43 (middle) or control vector (right), only primary (unilaminar) follicles were observed. Scale bars, 50 μm. Notice the different magnifications in the left, middle and right micrographs. (B) Distribution of follicle stages in the three different types of reaggregated ovaries as indicated below each group of bars. Between 22 and 72 follicles from three to four grafted ovaries were categorized for each group. A significant difference ($P<0.001$ wild type versus cys-less; $P<0.01$ wild type versus vector control, chi-square) was observed between ovaries expressing wild-type Cx43 and cys-less Cx43 in granulosa cells. Only the ovaries constructed with wild-type Cx43 were seen to contain antral follicles. (C) Expression of wild-type Cx43 and cys-less Cx43 in reaggregated ovaries. Infection was identified by EGFP expression (top row). Cx43 immunostaining (red, bottom row) showed mainly membrane expression of wild-type Cx43 with numerous gap junction-like plaques (left column) and predominately cytoplasmic localization of cys-less Cx43 (middle column). No Cx43 signal was detected in the empty-vector-infected ovaries (right column). Scale bar, 20 μm.

Table 2. Parameters for RT-PCR

Gene	Primer sequence	Annealing temperature (°C)	Amplicon size (bp)
Panx1	5′-TTCACTCTCGGACGAGTTTC-3′ 5′-TGGGCAGGATTTCATACACT-3′	56	227
Panx2	5′-CTGCTGCCTCTGAGAAAAAG-3′ 5′-GAGCAGACATGGAATGATCC-3′	56	276
Panx3	5′-ACACCATATTGGTCCCAGTG-3′ 5′-TGTCGATGTTGTGTTTCTGG-3′	62	252
P2rx7	5′-CGAGTTGGTGCCAGTGTGGA-3′ 5′-CCTGCTGTTGGTGGCCTCTT-3′	64	212
Actb	5′-CGTGGGCCGCCCTAGGCACCA-3′ 5′-TTGGCCTTAGGGTTCAGGGGGG-3′	56	243

junctional coupling. Cys-less Cx43 was targeted to the cell plasma membrane in both cases but had minimal capacity to mediate intercellular dye transfer, although it did convey gap junction hemichannel activity similar to wild-type Cx43 as demonstrated by dye uptake and ATP release in DCF medium. Therefore, this cys-less Cx43 construct provided a tool for testing the ability of undocked Cx43 hemichannels to rescue the folliculogenesis defect caused by the loss of Cx43 from granulosa cells, without the participation of intercellular gap junction channels.

An important issue is whether hemichannels have physiological or pathological functions in vivo. In this study, we delivered wild-type and cys-less Cx43 constructs into Cx43-deficient fetal pre-granulosa cells by retrovirus so that the constructs were stably integrated into the cell genome. This allowed them to be continually expressed during the 4-week period when the granulosa cells were proliferating in kidney grafts. By combining the granulosa cells with wild-type oocytes to make reaggregated ovaries, we evaluated the ability of the delivered constructs, expressed specifically in granulosa cells, to support folliculogenesis in vivo, simulating follicular development in the intact ovary. The efficiency of the retroviral delivery was proven by the successful expression of IRES-linked EGFP and ultimately by the ability of introduced Cx43 to advance folliculogenesis in the reaggregated ovaries made with Cx43-deficient granulosa cells. Therefore, the failure of cys-less Cx43-infected granulosa cells to support development beyond a very early follicle stage, a phenotype seen previously in Cx43-null mutant ovaries (Ackert et al., 2001), indicates that undocked Cx43 hemichannels cannot by themselves support normal granulosa cell function during folliculogenesis. In other words, intercellular gap junction channels composed of Cx43 are essential for follicle development in the mouse, whether or not undocked hemichannels also play a role. To our knowledge, this is the first study to evaluate possible contributions of gap junction hemichannels in vivo.

Materials and Methods

Animals

All animal experiments were approved by the Animal Use Subcommittee of the University Council on Animal Care at the University of Western Ontario. *Gja1*$^{-/-}$ C57BL/6 mice were produced by mating heterozygous mice. The genotype was determined by PCR as previously described (Gittens et al., 2005). To obtain follicles from mice lacking Cx43 (which die at birth), ovaries from late gestation fetuses [embryonic day (E)18.5] were collected and cultured in Waymouth's MB 752/1 medium (Invitrogen, Canada) containing 10% fetal bovine serum (FBS) (Invitrogen, Canada) on Millicell-PC (3.0 μm; 30 mm) polycarbonate membrane (Millipore, Bedford, MA) for 1 or 2 days until the genotypes of the ovary donors were determined. Ovaries were then grafted under kidney capsules of adult ovariectomized female severe combined immunodeficient (SCID) *Prkdc*^{scid}/*Prkdc*^{scid} mice (from Harlan Sprague Dawley, IN) as described previously (Gittens et al., 2003).

Cell culture

Follicles were isolated and cultured as described previously (Tong et al., 2006). Briefly, 20- to 24-day-old female mice or graft hosts 20-24 days after transplantation were anesthetized with CO_2 and killed by cervical dislocation. The ovaries were removed and placed in culture in Waymouth MB 752/1 medium containing 10% FBS, 100 U/ml penicillin and 100 μg/ml streptomycin (Invitrogen, Canada). Surrounding fat and connective tissue were removed using fine 30-gauge needles. The ovaries were then digested in medium containing 2 mg/ml type I collagenase (Sigma-Aldrich, Canada) to facilitate follicle release. Follicles were liberated by repeated aspiration and expulsion with a 1 ml pipettor. Care was taken to ensure that the follicles taken from wild-type ovaries were comparable in size to those from mutant mice. Follicles were washed with culture medium and transferred to another dish in which oocytes and granulosa cells were separated by treatment of trypsin-EDTA (0.05% trypsin, 0.53 mM EDTA tetrasodium salt, Invitrogen) for 5 minutes and centrifuged at 600 ***g*** for 5 minutes. The supernatant (containing oocytes) was removed and the granulosa cells resuspended in culture medium. They were transferred to 12 mm glass coverslips then cultured at 37°C in 5% CO_2/95% air for less than 48 hours.

Pre-granulosa cells were isolated from the ovaries of wild-type or mutant fetuses (gestation day 18.5) by dissociating with trypsin-EDTA for 45 minutes as previously described (Gittens and Kidder, 2005). Cell suspensions were centrifuged at 600 ***g*** for 5 minutes, resuspended in Medium 199 (M199) containing 10% FBS, 100 U/ml penicillin and 100 μg/ml streptomycin (Invitrogen, Canada), and cultured on 12 mm coverslips or 35 mm culture dishes at 37°C. The unattached oocytes were removed the next morning by changing the medium.

MDCK cells were maintained in DMEM (Invitrogen) containing 10% FBS, 100 U/ml penicillin and 100 μg/ml streptomycin at 37°C in 5% CO_2/95% air.

Dye-uptake assay

For each experiment, pooled wild-type or mutant granulosa cells from the ovaries of two to three mice were seeded on 12-mm glass coverslips in 24-well plates at a similar density of 30-40% confluency. For control conditions, cells were washed twice with regular extracellular solution (ECS) (142 mM NaCl, 5.4 mM KCl, 1.4 mM $MgCl_2$, 2 mM $CaCl_2$, 10 mM HEPES, 25 mM dextrose, osmolarity 298 mOsm, pH 7.35) and incubated for 15 minutes in 500 μl ECS containing 1% Lucifer yellow (LY, MW 457, Sigma-Aldrich). For DCF conditions, cells were washed once with regular ECS and once with DCF-ECS (Ca^{2+} and Mg^{2+} were replaced by 2 mM EGTA) and then incubated in 500 μl DCF-ECS containing 1% LY (with or without pharmacological blockers) for 15 minutes. All the blockers were pre-incubated in the DCF-ECS for 30 minutes. The incubation solution was then aspirated and the cells were washed three times with regular ECS, fixed with 4% paraformaldehyde and the nucleus was stained with Hoechst 33342. The coverslips were mounted on glass slides and images were captured on a Zeiss Axioskop 2 microscope equipped with a Retiga 1300 CCD digital camera (Q imaging). Cell counts were expressed as the percentage of cells loaded with LY relative to the total number of cells in view, counted after Hoechst staining. Between 30 and 100 cells were counted on each coverslip with three to six different experiments being performed for each experimental condition (i.e. n=3 or greater). In some experiments, as stated in the Results, 0.5 mM propidium iodide (PI, MW 668, Sigma-Aldrich) was used instead of LY. The osmolarity of all solutions was measured by an osmometer (Wescor Vapro 5520, Logan, Utah) and adjusted with dextrose.

Mechanical stimulation was achieved by gently pipetting ECS containing 10 mg/ml microglass beads (30-50 μm diameter, Polyscience) onto the cultured cells as described previously (Zhao et al., 2005). The solution containing 1% LY and glass beads with or without 200 μM carbenoxolone (CBX) was slowly pipetted with a 20 μl pipettor repeatedly during a 15-minute period. To exclude the possibility of cell membrane damage, rhodamine B dextran (5%, MW 10 kDa, Sigma-Aldrich) was added together with LY in one experiment (Fig. 1F). Cells were then washed, fixed and counted as described above. All experiments were performed at room temperature (23-25°C).

ATP measurement

Granulosa cells were treated as described above in regular or DCF ECS. Care was

taken that both wild-type and Cx43-deficient granulosa cells were seeded at the same density. The incubation solution was collected and the amount of ATP was measured by a bioluminescence-based method using a luciferin-luciferase assay kit (Invitrogen, Burlington, ON) and luminometer (Berthold Sirius D-75173, Pforzheim, Germany). ATP concentration in the incubation solution was calculated from a standard curve, which was simultaneously derived from serially eightfold-diluted ATP standards in each experiment. To minimize variation between experiments, each measurement was normalized to the baseline reading in the same experiment.

Semi-quantitative RT-PCR

RT-PCR was performed with RNA isolated from whole ovary, cultured pre-granulosa cells and granulosa cells using the RNeasy mini kit (Qiagen, Mississauga, ON). Total RNA (2 μg) was treated with DNase I (Invitrogen) and reverse transcribed using oligo(dT) primer with Superscript II reverse transcriptase (Invitrogen). The optimal number of PCR cycles was determined in advance for each primer pair using wild-type cDNA as template. *Actb* mRNA encoding β-actin served as an internal standard. The ideal ranges of PCR amplification observed were 33 cycles for *Panx1*, *Panx3* and *P2rx7*, 35 cycles for *Panx2*, and 26 cycles for *Actb*. Primer sequences and optimum annealing temperature for each PCR reaction are listed in Table 2. PCRs were performed in 25 μl volumes containing 2.5 μl 10× PCR buffer, 1 μl 50 mM $MgCl_2$, 3 μl 2 mM dNTP, 1 μl of each primer and 1 U Platinum Taq DNA polymerase (Invitrogen). Amplification was conducted with a Perkin Elmer 2400 thermal cycler as follows: initial denaturation for 10 minutes at 95°C followed by cycles of denaturation (30 seconds at 94°C), annealing (30 seconds at optimum temperature) and extension (1 minute at 72°C). Amplicons were visualized and quantified using Quantity One fluorescence detector and software (Bio-RAD, CA).

cDNA constructs

Rat Cx43 cDNA in Bluescript M13+ vector was amplified by oligonucleotides 5′-CCCTCGAGGGAAGGCGTGAGGAAAGTAC-3′ (RAT43F) and 5′-CGGGATCCAAGCCGGTTTAAATCTCCAG-3′ (RAT43R), which added a *Xho*I restriction site at the 5′ end and a *Bam*HI restriction site at the 3′ end of the cDNA. The amplified Cx43 cDNA was subcloned into pGEM-T Easy vector system I (Promega, Madison, WI). To generate cys-less Cx43 cDNA, all of the cysteine sites on the two extracellular loops (Fig. 3A) were mutated to alanine. A set of primers designed for the Quikchange multi-site-directed mutagenesis kit (Stratagene, La Jolla, CA) was used (mutated base underlined) in the mutant-strand synthesis reaction with the Cx43 cDNA in the pGEM-T Easy vector as template, as follows: 5′-CAGTCTGCCTTTCGCGCTAACACTCAACAACC-3′ (for Cys^{54}); 5′-ACTCAACAACCTGGCGCCGAAAACGTCGCCTATGACAAGTCCTTC-3′ (for Cys^{61} and Cys^{65}); 5′-CGCGGTCTACACCGCCAAGAGAGATCCCGCCCTCACCAGGTAG-3′ (for Cys^{187} and Cys^{192}); and 5′-CCTCACCAGGTAGACGCCTTCCTCTCACGTCC-3′ (for Cys^{198}). All of the oligonucleotides were purified by polyacrylamide gel electrophoresis. For the first mutant-strand synthesis reaction, primers for Cys^{54}, Cys^{187} and Cys^{192} were used to get the correspondent mutations. For the second reaction, the DNA product from the first reaction was used as template, and the primers were those for Cys^{61}, Cys^{65} and Cys^{198}. The cys-less Cx43 cDNA was released from the pGEM-T Easy vector using restriction endonucleases *Xho*I and *Bam*HI. The wild-type and cys-less Cx43 cDNAs were inserted into the AP2 retroviral vector, a murine plasmid retrovector including the enhanced green fluorescent protein (EGFP) reporter gene. The inserted cDNA and EGFP coding fragments were connected by an IRES to facilitate independent translation of the two proteins from the same mRNA (Fig. 3B) (Galipeau et al., 1999).

Retroviral infection of cells

The wild-type and cys-less Cx43 constructs were delivered into MDCK cells or Cx43-deficient granulosa cells by retrovirus as described previously (Qin et al., 2002). Briefly, the retroviral AP2 construct was transfected into 293GPG packaging cells using the LipofectAMINE PLUS procedure (Invitrogen, Canada). At 48 hours after transfection, 293GPG culture medium was replaced with fresh DMEM. Culture medium containing virus was collected daily for 7 consecutive days, filtered through a 0.45 μm syringe filter and concentrated by centrifugation (25,000 ***g***, 90 minutes) (Galipeau et al., 1999; Qin et al., 2002). The virus pellets concentrated from 5 ml of supernatant were resuspended in 200 μl medium. Cells grown to 40-50% confluency were incubated with concentrated retrovirus (200 μl virus was added into 2 ml culture medium) for 24 hours at 37°C. Infection efficiency was determined 48 hours after infection by visualizing live or fixed cells for EGFP expression under a fluorescence microscope.

Dye microinjection

LY (5%) was backfilled via capillary action through a 1 mm thin-wall glass capillary (World Precision Instruments, FL) pulled to a tip diameter of 1 μm. Clusters of EGFP-positive cells were selected for microinjection. One cell from each cluster was impaled and the dye was allowed to diffuse into the cell for 1 minute. After injection, recipient cells were counted. To avoid the possibility of cytoplasmic bridges, dye transfer was only scored as positive when the dye passed to more than one recipient cell.

Construction of reaggregated ovaries

Fetal ovaries were cultured as described above. Cx43-deficient ovaries were pooled (4-6 per group), washed with 1 mg/ml bovine serum albumin (BSA) (Sigma-Aldrich, Canada) in PBS and dissociated with 0.05% trypsin-EDTA for 45 minutes as previously described (Gittens and Kidder, 2005). Cell suspensions were centrifuged at 600 ***g*** for 5 minutes, resuspended in Medium 199 (M199) containing 10% FBS and transferred to tissue culture dishes (Easy Grip 35×10 mm, Falcon). Cells were cultured overnight in 5/5/90 atmosphere (5% CO_2, 5% O_2, 90% N_2) at 37°C. The following morning, unattached oocytes were removed and the pre-granulosa cells were incubated with retrovirus as described above for 24 hours. At the same time, ovaries from wild-type fetuses were dissociated and cells were cultured in the same way. After 6 hours of culture at 37°C in 5/5/90 atmosphere, the wild-type oocytes were collected and transferred to another culture dish for continuing culture, whereas the wild-type somatic cells were discarded. On the morning of the third day, the infected Cx43-deficient somatic cells were rinsed using 1 mg/ml BSA-PBS, dislodged from the dish with 0.05% trypsin-EDTA and centrifuged at 600 ***g*** for 5 minutes to pellet the cells. Wild-type oocytes were re-collected as described above, and pelleted by centrifuging at 600 ***g*** for 5 minutes. Wild-type oocytes were subjected to two rounds of seeding to avoid the contamination of wild-type somatic cells. Pellets were resuspended in 100 μl of M199/10% FBS with 7 μl/ml PHA lectin (0.05% phytohemagglutinin, Sigma-Aldrich). Wild-type oocytes and Cx43-deficient somatic cells infected with retrovirus were mixed and pelleted in a microfuge tube. Pellets were 'organ' cultured overnight in 5% CO_2 in air as described previously for fetal gonads (Gittens and Kidder, 2005). Chimeric ovaries were implanted beneath the renal capsules of bilaterally ovariectomized SCID mice as described above. Chimeric ovaries were harvested 28 days after the transplantation.

Histology and follicle counts

Chimeric ovaries were fixed in Bouin's solution, embedded in paraffin and sectioned at 5 μm. Sections were stained with hematoxylin and eosin. Follicles were counted and classified according to the number of layers of surrounding granulosa cells and the presence of an antrum. Care was taken that only follicles sectioned through the nucleus of the oocyte were counted. Three to four chimeric ovaries were examined for each group and three sections from each ovary were evaluated.

Immunofluorescence

Cells grown on coverslips were fixed with 4% paraformaldehyde for 20 minutes at room temperature. Coverslips were then washed three times with PBS and incubated for 1 hour in 2% BSA (Sigma-Aldrich) in PBS containing 0.1% Triton (Sigma-Aldrich). The Cx43 antibody was raised against the C-terminal tail of rat Cx43 (Sigma-Aldrich) and the secondary antibody was Alexa-Fluor-598-conjugated goat anti-rabbit IgG (Molecular Probes). Cell nuclei were labeled with Hoechst 33342 (1:1000 dilution; Molecular Probes). Coverslips were mounted on microscope slides using Airvol (Air Products and Chemicals, Allentown, PA) and imaged on a Zeiss (Thornwood, NY) LSM 510 META confocal microscope. Digital images were prepared using Zeiss LSM, Adobe Photoshop 7.0 and CorelDraw 12 software. For tissue sections, chimeric ovaries were fixed with 4% paraformaldehyde, embedded in paraffin and sectioned at 5 μm. Sections were de-waxed and stained with Cx43 antibody as described above.

Data analysis and statistics

The data are expressed as mean ± s.e.m., with '*n*' denoting the number of independent experiments. Comparison of two groups was carried out using a two-tailed unpaired *t*-test, with a *P* value below 0.05 indicating significance. Comparison of more than two groups was carried out with one-way ANOVA followed by a Tukey test. Two-way ANOVA and Bonferroni test were used to compare two groups under different experimental conditions. Statistical significance is indicated in the graphs with *** for $P<0.001$.

We are grateful to Kevin Barr for his expert advice, technical assistance and management of the mouse colony, and to the staff of the Health Sciences Animal Facility of the University of Western Ontario for daily care of the mice. We thank Dale Laird for providing the AP2 vector and 293GPG packaging cells, Jeffery Dixon for providing P2X7 receptor primers, Joanne Gittens for instructions on constructing reaggregated ovaries, and Qing Shao and Hong-Xing Wang for technical assistance. This research was funded by a grant to G.M.K. from the Canadian Institutes of Health Research (CIHR). D.B. is supported by the Canada Research Chairs program and D.T. is supported by a CIHR Doctoral Research Award.

References

Ackert, C. L., Gittens, J. E., O'Brien, M. J., Eppig, J. J. and Kidder, G. M. (2001). Intercellular communication via connexin43 gap junctions is required for ovarian folliculogenesis in the mouse. *Dev. Biol.* **233**, 258-270.

Bao, L., Locovei, S. and Dahl, G. (2004). Pannexin membrane channels are mechanosensitive conduits for ATP. *FEBS Lett.* **572**, 65-68.

Bao, X., Chen, Y., Reuss, L. and Altenberg, G. A. (2004). Functional expression in Xenopus oocytes of gap-junctional hemichannels formed by a cysteine-less connexin 43. *J. Biol. Chem.* **279**, 9689-9692.

Bennett, M. V., Contreras, J. E., Bukauskas, F. F. and Saéz, J. C. (2003). New roles for astrocytes: gap junction hemichannels have something to communicate. *Trends Neurosci.* **26**, 610-617.

Bruzzone, S., Guida, L., Zocchi, E., Franco, L. and De Flora, A. (2001). Connexin 43 hemi channels mediate Ca2+-regulated transmembrane NAD+ fluxes in intact cells. *FASEB J.* **15**, 10-12.

Cereijido, M., Robbins, E., Sabatini, D. D. and Stefani, E. (1984). Cell-to-cell communication in monolayers of epithelioid cells (MDCK) as a function of the age of the monolayer. *J. Membr. Biol.* **81**, 41-48.

Cherian, P. P., Siller-Jackson, A. J., Gu, S., Wang, X., Bonewald, L. F., Sprague, E. and Jiang, J. X. (2005). Mechanical strain opens connexin 43 hemichannels in osteocytes: a novel mechanism for the release of prostaglandin. *Mol. Biol. Cell* **16**, 3100-3106.

Dahl, G., Levine, E., Rabadan-Diehl, C. and Werner, R. (1991). Cell/cell channel formation involves disulfide exchange. *Eur. J. Biochem.* **197**, 141-144.

De Vuyst, E., Decrock, E., Cabooter, L., Dubyak, G. R., Naus, C. C., Evans, W. H. and Leybaert, L. (2006). Intracellular calcium changes trigger connexin 32 hemichannel opening. *EMBO J.* **25**, 34-44.

De Vuyst, E., Decrock, E., De Bock, M., Yamasaki, H., Naus, C. C., Evans, W. H. and Leybaert, L. (2007). Connexin hemichannels and gap junction channels are differentially influenced by lipopolysaccharide and basic fibroblast growth factor. *Mol. Biol. Cell* **18**, 34-46.

Flores, J. A., Aguirre, C., Sharma, O. P. and Veldhuis, J. D. (1998). Luteinizing hormone (LH) stimulates both intracellular calcium ion ([Ca2+]i) mobilization and transmembrane cation influx in single ovarian (granulosa) cells: recruitment as a cellular mechanism of LH-[Ca2+]i dose response. *Endocrinology* **139**, 3606-3612.

Galipeau, J., Li, H., Paquin, A., Sicilia, F., Karpati, G. and Nalbantoglu, J. (1999). Vesicular stomatitis virus G pseudotyped retrovector mediates effective in vivo suicide gene delivery in experimental brain cancer. *Cancer Res.* **59**, 2384-2394.

Gittens, J. E. and Kidder, G. M. (2005). Differential contributions of connexin37 and connexin43 to oogenesis revealed in chimeric reaggregated mouse ovaries. *J. Cell. Sci.* **118**, 5071-5078.

Gittens, J. E., Mhawi, A. A., Lidington, D., Ouellette, Y. and Kidder, G. M. (2003). Functional analysis of gap junctions in ovarian granulosa cells: distinct role for connexin43 in early stages of folliculogenesis. *Am. J. Physiol.* **284**, C880-C887.

Gittens, J. E., Barr, K. J., Vanderhyden, B. C. and Kidder, G. M. (2005). Interplay between paracrine signaling and gap junctional communication in ovarian follicles. *J. Cell. Sci.* **118**, 113-122.

Gomes, P., Srinivas, S. P., Van Driessche, W., Vereecke, J. and Himpens, B. (2005). ATP release through connexin hemichannels in corneal endothelial cells. *Invest. Ophthalmol. Vis. Sci.* **46**, 1208-1218.

Goodenough, D. A. and Paul, D. L. (2003). Beyond the gap: functions of unpaired connexon channels. *Nat. Rev. Mol. Cell Biol.* **4**, 285-294.

Hibell, A. D., Thompson, K. M., Xing, M., Humphrey, P. P. and Michel, A. D. (2001). Complexities of measuring antagonist potency at P2X(7) receptor orthologs. *J. Pharmacol. Exp. Ther.* **296**, 947-957.

Huang, Y. J., Maruyama, Y., Dvoryanchikov, G., Pereira, E., Chaudhari, N. and Roper, S. D. (2007). The role of pannexin 1 hemichannels in ATP release and cell-cell communication in mouse taste buds. *Proc. Natl. Acad. Sci. USA* **104**, 6436-6441.

Jiang, J. X. and Gu, S. (2005). Gap junction- and hemichannel-independent actions of connexins. *Biochim. Biophys. Acta* **1711**, 208-214.

Kamada, S., Blackmore, P. F., Kubota, T., Oehninger, S., Asada, Y., Gordon, K., Hodgen, G. D. and Aso, T. (1995). The role of endothelin-1 in regulating human granulosa cell proliferation and steroidogenesis in vitro. *J. Clin. Endocrinol. Metab.* **80**, 3708-3714.

Kidder, G. M. (2005). Roles of gap junctions in ovarian folliculogenesis: implications for female infertility. In *Gap Junctions in Development and Disease* (ed. E. Winterhager), pp 223-237. Heidelberg, Germany: Springer Verlag.

Lai, A., Le, D. N., Paznekas, W. A., Gifford, W. D., Jabs, E. W. and Charles, A. C. (2006). Oculodentodigital dysplasia connexin43 mutations result in non-functional connexin hemichannels and gap junctions in C6 glioma cells. *J. Cell. Sci.* **119**, 532-541.

Lara, H. E., Porcile, A., Espinoza, J., Romero, C., Luza, S. M., Fuhrer, J., Miranda, C. and Roblero, L. (2001). Release of norepinephrine from human ovary: coupling to steroidogenic response. *Endocrine* **15**, 187-192.

Li, H., Liu, T. F., Lazrak, A., Peracchia, C., Goldberg, G. S., Lampe, P. D. and Johnson, R. G. (1996). Properties and regulation of gap junctional hemichannels in the plasma membranes of cultured cells. *J. Cell Biol.* **134**, 1019-1030.

Nandi, S., Kumar, V. G. and Gupta, P. S. (2006). Effect of ovine follicular fluid peptide on ovarian responses and other organ weights in rats, Rattus norvegicus berkenhout 1769. *Indian J. Exp. Biol.* **44**, 880-885.

Park, D. W., Cho, T., Kim, M. R., Kim, Y. A., Min, C. K. and Hwang, K. J. (2003). ATP-induced apoptosis of human granulosa luteal cells cultured in vitro. *Fertil. Steril.* **80**, 993-1002.

Pelegrin, P. and Surprenant, A. (2006). Pannexin-1 mediates large pore formation and interleukin-1beta release by the ATP-gated P2X7 receptor. *EMBO J.* **25**, 5071-5082.

Plotkin, L. I., Manolagas, S. C. and Bellido, T. (2002). Transduction of cell survival signals by connexin-43 hemichannels. *J. Biol. Chem.* **277**, 8648-8657.

Qin, H., Shao, Q., Curtis, H., Galipeau, J., Belliveau, D. J., Wang, T., Alaoui-Jamali, M. A. and Laird, D. W. (2002). Retroviral delivery of connexin genes to human breast tumor cells inhibits in vivo tumor growth by a mechanism that is independent of significant gap junctional intercellular communication. *J. Biol. Chem.* **277**, 29132-29138.

Quist, A. P., Rhee, S. K., Lin, H. and Lal, R. (2000). Physiological role of gap-junctional hemichannels. extracellular calcium-dependent isosmotic volume regulation. *J. Cell Biol.* **148**, 1063-1074.

Söhl, G. and Willecke, K. (2004). Gap junctions and the connexin protein family. *Cardiovasc. Res.* **62**, 228-232.

Stout, C. E., Costantin, J. L., Naus, C. C. and Charles, A. C. (2002). Intercellular calcium signaling in astrocytes via ATP release through connexin hemichannels. *J. Biol. Chem.* **277**, 10482-10488.

Suadicani, S. O., Brosnan, C. F. and Scemes, E. (2006). P2X7 receptors mediate ATP release and amplification of astrocytic intercellular Ca2+ signaling. *J. Neurosci.* **26**, 1378-1385.

Tai, C. J., Kang, S. K., Cheng, K. W., Choi, K. C., Nathwani, P. S. and Leung, P. C. (2000). Expression and regulation of P2U-purinergic receptor in human granulosa-luteal cells. *J. Clin. Endocrinol. Metab.* **85**, 1591-1597.

Tong, D., Gittens, J. E., Kidder, G. M. and Bai, D. (2006). Patch-clamp study reveals that the importance of connexin43-mediated gap junctional communication for ovarian folliculogenesis is strain specific in the mouse. *Am. J. Physiol.* **290**, C290-C297.

Webb, R. J., Bains, H., Cruttwell, C. and Carroll, J. (2002). Gap-junctional communication in mouse cumulus-oocyte complexes: Implications for the mechanism of meiotic maturation. *Reproduction* **123**, 41-52.

Ye, Z. C., Wyeth, M. S., Baltan-Tekkok, S. and Ransom, B. R. (2003). Functional hemichannels in astrocytes: a novel mechanism of glutamate release. *J. Neurosci.* **23**, 3588-3596.

Zhao, H. B., Yu, N. and Fleming, C. R. (2005). Gap junctional hemichannel-mediated ATP release and hearing controls in the inner ear. *Proc. Natl. Acad. Sci. USA* **102**, 18724-18729.